*Journal of Sound and Vibration* (2000) **237**(3), 377–393
doi:10.1006/jsvi.2000.3030, available online at http://www.idealibrary.com on IDEAL®

# MODAL INTERACTIONS OF A RANDOMLY EXCITED HINGED–CLAMPED BEAM

D. S. Cho

*Institute of Industrial Technology, Yeungnam University, Gyongsan* 712-749, *Korea*

AND

W. K. Lee

*Department of Mechanical Engineering, Yeungnam University, Gyongsan* 712-749, *Korea*

(*Received* 29 *June* 1999, *and in final form* 10 *March* 2000)

An investigation into the response statistics of a hinged–clamped beam under broadband random excitation is made. By using Galerkin's method the governing equation is reduced to a system of non-autonomous non-linear ordinary differential equations. The Fokker–Planck equation is applied to generate a general first order differential equation in the dynamic moments of response co-ordinates. By means of the Gaussian and non-Gaussian closure methods the dynamic moment equations for the random responses of the system are reduced to a system of autonomous ordinary differential equations. The analytical results for two- and three-mode interactions are also compared with results obtained by Monte Carlo simulation.



## 1. INTRODUCTION

A straight beam with fixed ends experiences mid-plane stretching when deflected. The influence of this stretching on the dynamic response increases with the amplitude of the response. This situation can be described with non-linear strain–displacement equations and a linear stress–strain law which give us the non-linear beam equation. Even though a beam is a continuous system, it can be approximated as a multi-degree-of-freedom system. When a non-linear multi-degree-of-freedom system has two or more of its natural frequencies commensurable or nearly so, the system may possess internal resonances (modal interactions).

Non-linear dynamic responses of simply supported or clamped beams have been studied by many authors [1–12]. Under harmonic excitation, Nayfeh and his colleagues [5–7], and Lee and his colleagues [8–10] considered two- or three-mode interaction to study the steady state responses of a hinged–clamped beam. Lee and Soh [8] showed that there exists no significant difference between two and three-mode interactions' influences on the responses.

On the other hand, Ibrahim and his colleagues [11, 12] have studied the stochastic bifurcation of the unexcited mode of a clamped–clamped beam under wide band random excitation when initial static axial load is applied to the beam. When the load does not exceed the Euler buckling load [11], the Gaussian closure failed to predict bifurcation of unexcited second mode under all possible conditions of axial load and excitation level. But both the non-Gaussian closure and Monte Carlo simulation predicted second mode

0022-460X/00/430377 + 17 $35.00/0 

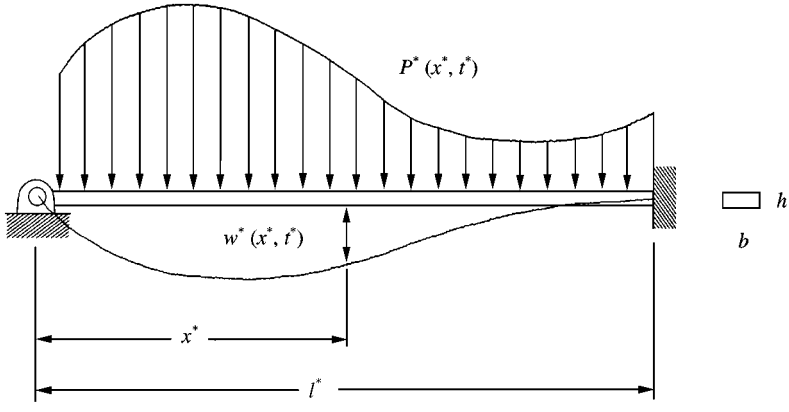


Figure 1. A schematic diagram of a hinged–clamped beam.

bifurcation. When the load exceeds the Euler buckling load [12], the Gaussian closure method and Monte Carlo simulation give almost consistent bifurcation points of the second mode, which are inconsistent with the non-Gaussian closure result.

In this study, to investigate influences of the internal resonance of a hinged–clamped beam with a random excitation we reduce a partial differential equation of motion and boundary conditions to a system of coupled non-linear ordinary differential equations using Galerkin's procedure. Obtaining moment equations from the Fokker–Planck equation corresponding to the coupled non-linear ordinary differential equations, we used Gaussian and non-Gaussian closure schemes to reduce a system of autonomous ordinary differential equations for moments. The response statistics of these systems are examined. We consider two- and three-mode interactions by the Gaussian closure scheme, and two-mode interaction by the non-Gaussian closure scheme. The results obtained by two closure schemes are compared with those obtained by Monte Carlo simulation.

## 2. EQUATION OF MOTION FOR BEAM

Consider a slender, initially straight hinged–clamped beam, which is shown in Figure 1. For such a beam, the partial differential equation of motion and boundary conditions can be represented as follows [5]:

$$EI\frac{\partial^4 w^*}{\partial x^{*4}} + \rho A\frac{\partial^2 w^*}{\partial t^{*2}} = -2c^*\frac{\partial w^*}{\partial t^*} + H^*\frac{\partial^2 w^*}{\partial x^{*2}} + P^*(x^*, t^*),$$

$$w^*(0, t^*) = 0, \quad \frac{\partial^2 w^*(0, t^*)}{\partial x^{*2}} = 0,$$

$$w^*(l^*, t^*) = 0, \quad \frac{\partial w^*(l^*, t^*)}{\partial x^*} = 0,$$

where $E$ is the Young's modulus, $b$ the width of beam, $h$ the thickness of beam, $\rho$ the density of beam, $I(= bh^3/12)$ the area moment of inertia, $c^*$ the damping coefficient, $P^*$ the exciting random force, $H^*(= EA/2l^*\int_0^{l^*}(\partial w^*/\partial x^*)^2\,\mathrm{d}x^*)$ the tension due to mid-plane stretching,

$w^*$ the deflection of the beam, $t^*$ the time in seconds, $x^*$ the longitudinal axis, $l^*$ the length of the beam, and $A$ the cross-sectional area of the beam.

Rewriting the equations in terms of dimensionless variables, we have

$$\frac{\partial^4 w}{\partial x^4} + \frac{\partial^2 w}{\partial t^2} = \varepsilon\left[ -2c\,\frac{\partial w}{\partial t} + H\,\frac{\partial^2 w}{\partial x^2} + P \right].$$

$$w(0, t) = 0, \quad \frac{\partial^2 w(0, t)}{\partial x^2} = 0,$$

$$w(l, t) = 0, \quad \frac{\partial w(l, t)}{\partial x} = 0, \tag{1}$$

where $H = v\int_0^l (\partial w/\partial x)^2\,\mathrm{d}x$, $v = 1/2l$, $x^* = xL$, $L = l^*/2$, $l = l^*/L = 2$, $r = (I/A)^{1/2}$ = radius of gyration, $t^* = (\rho L^4/Er^2)^{1/2}t$, $w^* = r^2 w/L$, $\varepsilon = r^2/L^2 = (h/L)^2/12$, $P^* = (r^6 EA/L^7)P$, $c^* = 2cr^3 A(\rho E)^{1/2}/L^4$, and $H^* = EAH(r/L)^4$.

Equation (1) can be solved approximately by Galerkin's method. The deflection is approximated by

$$w(x, t) = \sum_{n=1}^{\infty} u_n(t)\,\varphi_n(x), \tag{2}$$

where $u_n$ are generalized co-ordinates and $\varphi_n$ are eigenfunctions of the following eigenvalue problem:

$$\frac{\mathrm{d}^4 \varphi_n}{\mathrm{d}x^4} - \omega_n^2 \varphi_n = 0,$$

$$\varphi_n(0) = 0, \quad \frac{\mathrm{d}^2 \varphi_n(0)}{\mathrm{d}x^2} = 0, \qquad \varphi_n(l) = 0, \quad \frac{\mathrm{d}\varphi_n(l)}{\mathrm{d}x} = 0, \tag{3}$$

where $\omega_n$ are natural frequencies. The eigenfunction of the eigenvalue problem (3) is

$$\varphi_n = e_n[\sin(\alpha_n x) - R_n \sinh(\alpha_n x)], \tag{4}$$

where

$$e_n = [\tfrac{1}{2}\,l(l - R_n^2) + \{R_n^2 \sinh(2\alpha_n l) - \sin(2\alpha_n l)\}/(4\alpha_n)]^{-1/2},$$

$$R_n = \sin(\alpha_n l)/\sinh(\alpha_n l), \qquad \alpha_n = \omega_n^{1/2},$$

and $\alpha_n$ are the roots of $\tan(\alpha_n l) = \tanh(\alpha_n l)$. The first three eigenfunctions are shown in Figure 2. Since $l = 2$, the first three roots and frequencies are

$$\alpha_1 l = 3{\cdot}927 \quad \text{and} \quad \omega_1 = 3{\cdot}855, \qquad \alpha_2 l = 7{\cdot}069 \quad \text{and} \quad \omega_2 = 12{\cdot}491,$$

$$\alpha_3 l = 10{\cdot}210 \quad \text{and} \quad \omega_3 = 26{\cdot}062.$$

From the observation of these natural frequencies, we can see the relations $\omega_2 \approx 3\omega_1$ and $\omega_3 \approx \omega_1 + 2\omega_2$, which satisfy the internal resonance condition. Substituting Eq. (2) into Eq. (1), multiplying by $\varphi_m$, integrating over the length, and using the orthogonality of the eigenfunctions we obtain a set of non-linear ordinary differential

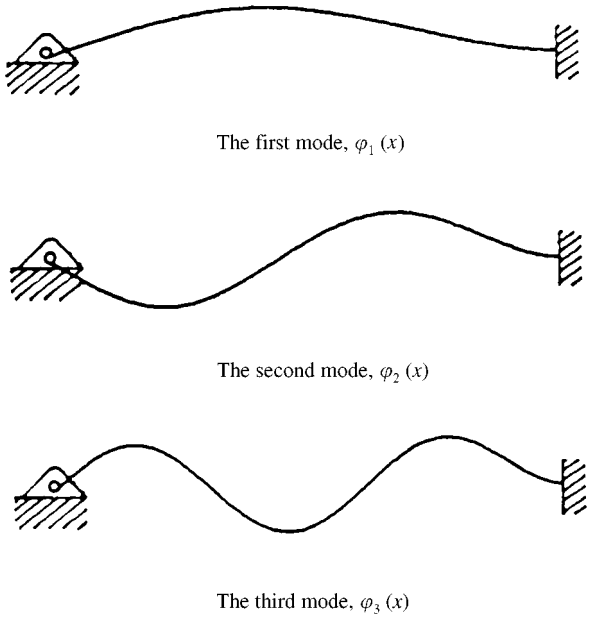


Figure 2. Eigenfunctions of the beam vibration.

equations

$$\frac{d^2u_n}{dt^2} + \omega_n^2 u_n = \varepsilon\Big[ -2c_n \frac{du_n}{dt} + s_{n0}u_1^3 + s_{n1}u_1^2u_2 + s_{n2}u_1u_2^2 + s_{n3}u_2^3 + s_{n4}u_1^2u_3 + s_{n5}u_1u_2u_3 + s_{n6}u_2^2u_3 + s_{n7}u_1u_3^2 + s_{n8}u_2u_3^2 + s_{n9}u_3^3 + F_n(t)\Big], \quad n = 1, 2, 3, \tag{5}$$

where

$s_{10} = -2{\cdot}071$, $s_{11} = -2{\cdot}311$, $s_{12} = -8{\cdot}289$, $s_{13} = -2{\cdot}870$, $s_{14} = 2{\cdot}050$

$s_{15} = -1{\cdot}796$, $s_{16} = 1{\cdot}450$, $s_{17} = -17{\cdot}367$, $s_{18} = -5{\cdot}364$, $s_{19} = 5{\cdot}581$

$s_{20} = -0{\cdot}770$, $s_{21} = -8{\cdot}289$, $s_{22} = -8{\cdot}610$, $s_{23} = -28{\cdot}752$, $s_{24} = -0{\cdot}898$

$s_{25} = 2{\cdot}999$, $s_{26} = -15{\cdot}722$, $s_{27} = -5{\cdot}364$, $s_{28} = -64{\cdot}940$, $s_{29} = -11{\cdot}489$

$s_{30} = 0{\cdot}683$, $s_{31} = -0{\cdot}898$, $s_{32} = 1{\cdot}450$, $s_{33} = -5{\cdot}241$, $s_{34} = -17{\cdot}367$

$s_{35} = -10{\cdot}728$, $s_{36} = -64{\cdot}940$, $s_{37} = 16{\cdot}744$, $s_{38} = -34{\cdot}467$, $s_{39} = -138{\cdot}173$

$$c_n = \int_0^l c\varphi_n^2 \, dx, \qquad F_n(t) = \int_0^l P(x, t)\, \varphi_n \, dx.$$

In this study we consider two cases of excitations.

*Case* I: When the excitation is applied at the nodal point of the second mode (indirectly excited second mode).

To investigate the influences of the energy transfer from the directly excited modes ($u_1$, $u_3$) to the indirectly excited mode ($u_2$) through non-linear coupling, we select the nodal point of the second mode as an excitation point. Letting the second natural mode be zero, i.e.,

$$\varphi_2 = e_2[\sin(\alpha_2 x_W) - R_2 \sinh(\alpha_2 x_W)] = 0,$$

then we can find $x_W = 0{\cdot}885$. In this case, the random excitations corresponding to three modes are, respectively, as follows:

$$F_1(t) = \int_0^l \delta(x - x_W)\,\varphi_1(x)\,W(t)\,\mathrm{d}x = f_1 W(t),$$

$$F_2(t) = \int_0^l \delta(x - x_W)\,\varphi_2(x)\,W(t)\,\mathrm{d}x = f_2 W(t),$$

$$F_3(t) = \int_0^l \delta(x - x_W)\,\varphi_3(x)\,W(t)\,\mathrm{d}x = f_3 W(t), \tag{6}$$

where

$$W(t) = P(0{\cdot}885, t), \qquad f_1 = \varphi_1(x_W) = 1{\cdot}063, \qquad f_2 = \varphi_2(x_W) = 0,$$

$$f_3 = \varphi_3(x_W) = -0{\cdot}979. \tag{7}$$

*Case* II: When the excitation is applied at the antinode of the second mode (directly excited second mode).

In order to excite directly the second mode, we select the antinode of the second mode as excitation point. Letting first derivative of the second natural mode be zero, i.e.,

$$\left.\frac{\mathrm{d}\varphi_2(x)}{\mathrm{d}x}\right|_{x = x_W} = 0$$

then we can find $x_W = 1{\cdot}354$. In this case, the coefficients of the random excitation corresponding to three modes are as follows:

$$f_1 = \varphi_1(x_W) = 0{\cdot}663, \qquad f_2 = \varphi_2(x_W) = -1{\cdot}069, \qquad f_3 = \varphi_3(x_W) = 0{\cdot}613. \tag{8}$$

Random excitation $W(t)$ is assumed to be zero mean white noise having the autocorrelation function

$$R_{WW}(\Delta t) = E[W(t)\,W(t + \Delta t)] = 2D\delta(\Delta t), \tag{9}$$

where $2D$ represents the spectral density when we express the frequency by $f\,(= \omega/2\pi)$, and $\delta(\Delta t)$ is the Dirac delta function.

## 3. FOKKER–PLANCK EQUATION

Introducing the notations

$$\{u_1, u_1', u_2, u_2', u_3, u_3'\}^{\mathrm{T}} = \{X_1, X_2, X_3, X_4, X_5, X_6\}^{\mathrm{T}} = \mathbf{X},$$

where prime denotes differentiation with respect to $t$, and letting $W(t)$ be a formal derivative of a Brownian process, i.e., $W(t) = \mathrm{d}B(t)/\mathrm{d}t$, we can express the equations (5) as following Ito stochastic differential equation:

$$\begin{aligned}
\mathrm{d}X_1 &= X_2\,\mathrm{d}t,\\
\mathrm{d}X_2 &= [-\omega_1^2 X_1 + \varepsilon(-2c_1X_2 + s_{10}X_1^3 + s_{11}X_1^2X_3 + s_{12}X_1X_3^2\\
&\quad + s_{13}X_3^3 + s_{14}X_1^2X_5 + s_{15}X_1X_3X_5 + s_{16}X_3^2X_5\\
&\quad + s_{17}X_1X_5^2 + s_{18}X_3X_5^2 + s_{19}X_5^3)]\,\mathrm{d}t + \varepsilon f_1\,\mathrm{d}B,\\
\mathrm{d}X_3 &= X_4\,\mathrm{d}t,\\
\mathrm{d}X_4 &= [-\omega_2^2 X_3 + \varepsilon(-2c_2X_4 + s_{20}X_1^3 + s_{21}X_1^2X_3 + s_{22}X_1X_3^2\\
&\quad + s_{23}X_3^3 + s_{24}X_1^2X_5 + s_{25}X_1X_3X_5 + s_{26}X_3^2X_5\\
&\quad + s_{27}X_1X_5^2 + s_{28}X_3X_5^2 + s_{29}X_5^3)]\,\mathrm{d}t + \varepsilon f_2\,\mathrm{d}B,\\
\mathrm{d}X_5 &= X_6\,\mathrm{d}t,\\
\mathrm{d}X_6 &= [-\omega_3^2 X_5 + \varepsilon(-2c_3X_6 + s_{30}X_1^3 + s_{31}X_1^2X_3 + s_{32}X_1X_3^2\\
&\quad + s_{33}X_3^3 + s_{34}X_1^2X_5 + s_{35}X_1X_3X_5 + s_{36}X_3^2X_5\\
&\quad + s_{37}X_1X_5^2 + s_{38}X_3X_5^2 + s_{39}X_5^3)]\,\mathrm{d}t + \varepsilon f_3\,\mathrm{d}B. \qquad (10)
\end{aligned}$$

The solution process of this equation is a Markov process and the Fokker–Planck equation may be applied for the Markov vector $\mathbf{X}$ in the form

$$\begin{aligned}
\frac{\partial}{\partial t}p(\mathbf{x}, t) &= -\sum_{j=1}^{6}\frac{\partial}{\partial x_j}[a_j(\mathbf{x}, t)\,p(\mathbf{x}, t)]\\
&\quad + \frac{1}{2}\sum_{j=1}^{6}\sum_{k=1}^{6}\frac{\partial^2}{\partial x_j\,\partial x_k}[b_{jk}(\mathbf{x}, t)\;p(\mathbf{x}, t)], \qquad (11)
\end{aligned}$$

where $p(\mathbf{x}, t)$ is the joint probability density function, and $a_j(\mathbf{x}, t)$ and $b_{jk}(\mathbf{x}, t)$ are the first and second incremental moments of the Markov process $\mathbf{X}(t)$, and $x_j$ are the component of $\mathbf{x}$. These incremental moments are defined as follows [13]:

$$a_j(\mathbf{x}, t) = \lim_{\delta t \to 0}\frac{1}{\delta t}E\{X_j(t+\delta t) - X_j(t)\,|\,\mathbf{X}(t) = \mathbf{x}\}, \qquad (12)$$

$$\begin{aligned}
b_{jk}(\mathbf{x}, t) &= \lim_{\delta t \to 0}\frac{1}{\delta t}E\{[X_j(t+\delta t) - X_j(t)]\\
&\quad \times [X_k(t+\delta t) - X_k(t)]\,|\,\mathbf{X}(t) = \mathbf{x}\}. \qquad (13)
\end{aligned}$$

## 4. MOMENT EQUATIONS

Since it is impossible to obtain the exact solution $p(\mathbf{x}, t)$ to the Fokker–Planck equation [14, 15], we are trying to examine the system responses by means of moment equations. First of all, introducing the following notations for the $n$th order moments of the system responses:

$$m_{\beta_1,\beta_2,\beta_3,\beta_4,\beta_5,\beta_6}(t) = E[X_1^{\beta_1} X_2^{\beta_2} X_3^{\beta_3} X_4^{\beta_4} X_5^{\beta_5} X_6^{\beta_6}]$$

$$= \int\int\int\int\int\int_{-\infty}^{\infty} x_1^{\beta_1} x_2^{\beta_2} x_3^{\beta_3} x_4^{\beta_4} x_5^{\beta_5} x_6^{\beta_6} p(\mathbf{x}, t)\, dx_1\, dx_2\, dx_3\, dx_4\, dx_5\, dx_6$$

with $n = \beta_1 + \beta_2 + \beta_3 + \beta_4 + \beta_5 + \beta_6$, we can derive a set of dynamic moment equations of any order by multiplying equation (11) by $x_1^{\beta_1} x_2^{\beta_2} x_3^{\beta_3} x_4^{\beta_4} x_5^{\beta_5} x_6^{\beta_6}$ and integrating by parts over the entire state space $-\infty < x_i < \infty$. This procedure results in the following general dynamic moment equation:

$$\begin{aligned}
m'_{\beta_1,\beta_2,\beta_3,\beta_4,\beta_5,\beta_6} = {} & \beta_1 m_{\beta_1-1,\beta_2+1,\beta_3,\beta_4,\beta_5,\beta_6} - \beta_2\omega_1^2 m_{\beta_1+1,\beta_2-1,\beta_3,\beta_4,\beta_5,\beta_6} \\
& + \beta_3 m_{\beta_1,\beta_2,\beta_3-1,\beta_4+1,\beta_5,\beta_6} - \beta_4\omega_2^2 m_{\beta_1,\beta_2,\beta_3+1,\beta_4-1,\beta_5,\beta_6} \\
& + \beta_5 m_{\beta_1,\beta_2,\beta_3,\beta_4,\beta_5-1,\beta_6+1} - \beta_6\omega_3^2 m_{\beta_1,\beta_2,\beta_3,\beta_4,\beta_5+1,\beta_6-1} \\
& + \varepsilon s_{10}\beta_2 m_{\beta_1+3,\beta_2-1,\beta_3,\beta_4,\beta_5,\beta_6} - 2\varepsilon c_1\beta_2 m_{\beta_1,\beta_2,\beta_3,\beta_4,\beta_5,\beta_6} \\
& + \varepsilon s_{11}\beta_2 m_{\beta_1+2,\beta_2-1,\beta_3+1,\beta_4,\beta_5,\beta_6} + \varepsilon s_{12}\beta_2 m_{\beta_1+1,\beta_2-1,\beta_3+2,\beta_4,\beta_5,\beta_6} \\
& + \varepsilon s_{13}\beta_2 m_{\beta_1,\beta_2-1,\beta_3+3,\beta_4,\beta_5,\beta_6} + \varepsilon s_{14}\beta_2 m_{\beta_1+2,\beta_2-1,\beta_3+3,\beta_4,\beta_5+1,\beta_6} \\
& + \varepsilon s_{15}\beta_2 m_{\beta_1+1,\beta_2-1,\beta_3+1,\beta_4,\beta_5+1,\beta_6} + \varepsilon s_{16}\beta_2 m_{\beta_1,\beta_2-1,\beta_3+2,\beta_4,\beta_5+1,\beta_6} \\
& + \varepsilon s_{17}\beta_2 m_{\beta_1+1,\beta_2-1,\beta_3,\beta_4,\beta_5+2,\beta_6} + \varepsilon s_{18}\beta_2 m_{\beta_1,\beta_2-1,\beta_3+1,\beta_4,\beta_5+2,\beta_6} \\
& + \varepsilon s_{19}\beta_2 m_{\beta_1,\beta_2-1,\beta_3,\beta_4,\beta_5+3,\beta_6} \\
& + \varepsilon s_{20}\beta_4 m_{\beta_1+3,\beta_2,\beta_3,\beta_4-1,\beta_5,\beta_6} - 2\varepsilon c_2\beta_4 m_{\beta_1,\beta_2,\beta_3,\beta_4,\beta_5,\beta_6} \\
& + \varepsilon s_{21}\beta_4 m_{\beta_1+2,\beta_2,\beta_3+1,\beta_4-1,\beta_5,\beta_6} + \varepsilon s_{22}\beta_4 m_{\beta_1+1,\beta_2,\beta_3+2,\beta_4-1,\beta_5,\beta_6} \\
& + \varepsilon s_{23}\beta_4 m_{\beta_1,\beta_2,\beta_3+3,\beta_4-1,\beta_5,\beta_6} + \varepsilon s_{24}\beta_4 m_{\beta_1+2,\beta_2,\beta_3+3,\beta_4-1,\beta_5+1,\beta_6} \\
& + \varepsilon s_{25}\beta_4 m_{\beta_1+1,\beta_2,\beta_3+1,\beta_4-1,\beta_5+1,\beta_6} + \varepsilon s_{26}\beta_4 m_{\beta_1,\beta_2,\beta_3+2,\beta_4-1,\beta_5+1,\beta_6} \\
& + \varepsilon s_{27}\beta_4 m_{\beta_1+1,\beta_2,\beta_3,\beta_4-1,\beta_5+2,\beta_6} + \varepsilon s_{28}\beta_4 m_{\beta_1,\beta_2,\beta_3+1,\beta_4-1,\beta_5+2,\beta_6} \\
& + \varepsilon s_{29}\beta_4 m_{\beta_1,\beta_2,\beta_3,\beta_4-1,\beta_5+3,\beta_6}
\end{aligned}$$

$$
\begin{aligned}
&+ \varepsilon s_{30}\beta_6 m_{\beta_1+3,\beta_2,\beta_3,\beta_4,\beta_5,\beta_6-1} - 2\varepsilon c_3\beta_6 m_{\beta_1,\beta_2,\beta_3,\beta_4,\beta_5,\beta_6}\\
&+ \varepsilon s_{31}\beta_6 m_{\beta_1+2,\beta_2,\beta_3+1,\beta_4,\beta_5,\beta_6-1} + \varepsilon s_{32}\beta_6 m_{\beta_1+1,\beta_2,\beta_3+2,\beta_4,\beta_5,\beta_6-1}\\
&+ \varepsilon s_{33}\beta_6 m_{\beta_1,\beta_2,\beta_3+3,\beta_4,\beta_5,\beta_6-1} + \varepsilon s_{34}\beta_6 m_{\beta_1+2,\beta_2,\beta_3+3,\beta_4,\beta_5+1,\beta_6-1}\\
&+ \varepsilon s_{35}\beta_6 m_{\beta_1+1,\beta_2,\beta_3+1,\beta_4,\beta_5+1,\beta_6-1} + \varepsilon s_{36}\beta_6 m_{\beta_1,\beta_2,\beta_3+2,\beta_4,\beta_5+1,\beta_6-1}\\
&+ \varepsilon s_{37}\beta_6 m_{\beta_1+1,\beta_2,\beta_3,\beta_4,\beta_5+2,\beta_6-1} + \varepsilon s_{38}\beta_6 m_{\beta_1,\beta_2,\beta_3+1,\beta_4,\beta_5+2,\beta_6-1}\\
&+ \varepsilon s_{39}\beta_6 m_{\beta_1,\beta_2,\beta_3,\beta_4,\beta_5+3,\beta_6-1}\\
&+ \varepsilon^2\beta_2(\beta_2-1) f_1^2 Dm_{\beta_1,\beta_2-2,\beta_3,\beta_4,\beta_5,\beta_6}\\
&+ \varepsilon^2\beta_4(\beta_4-1) f_2^2 Dm_{\beta_1,\beta_2,\beta_3,\beta_4-2,\beta_5,\beta_6}\\
&+ \varepsilon^2\beta_6(\beta_6-1) f_3^2 Dm_{\beta_1,\beta_2,\beta_3,\beta_4,\beta_5,\beta_6-2}\\
&+ 2\beta_2\beta_4 f_1 f_2 Dm_{\beta_1,\beta_2-1,\beta_3,\beta_4-1,\beta_5,\beta_6}\\
&+ 2\beta_2\beta_6 f_1 f_3 Dm_{\beta_1,\beta_2-1,\beta_3,\beta_4,\beta_5,\beta_6-1}\\
&+ 2\beta_4\beta_6 f_2 f_3 Dm_{\beta_1,\beta_2,\beta_3,\beta_4-1,\beta_5,\beta_6-1} \qquad (14)
\end{aligned}
$$

## 5. CLOSURE SCHEMES

Equation (14) constitutes a set of infinite coupled equations. In other words, the differential equation of order $n$ contains moment terms of orders $n+1$ and $n+2$. In order to solve for response statistics these equations must be truncated by an appropriate closure scheme. Two cumulant truncation schemes are used. These are the Gaussian and non-Gaussian closures.

The Gaussian closure is based on the assumption that the response process is nearly Gaussian and is carried out by setting third and fourth order cumulants to zero. In this case, we can generate 14 coupled differential equations for first and second order moments depend on the first through fourth moments. The third and fourth order moments can be expressed in terms of lower order moments as follows:

$$E[X_{h_1}X_{h_2}X_{h_3}] = \sum^{3} E[X_{h_1}]\,E[X_{h_2}X_{h_3}] - 2E[X_{h_1}]\,E[X_{h_2}]\,E[X_{h_3}], \qquad (15)$$

$$
\begin{aligned}
E[X_{h_1}X_{h_2}X_{h_3}X_{h_4}] = &\sum^{4} E[X_{h_1}]\,E[X_{h_2}X_{h_3}X_{h_4}]\\
&- 2\sum^{6} E[X_{h_1}]\,E[X_{h_2}]\,E[X_{h_3}X_{h_4}]\\
&+ \sum^{3} E[X_{h_1}X_{h_2}]\,E[X_{h_3}X_{h_4}]\\
&+ 6E[X_{h_1}]\,E[X_{h_2}]\,E[X_{h_3}]\,E[X_{h_4}]. \qquad (16)
\end{aligned}
$$

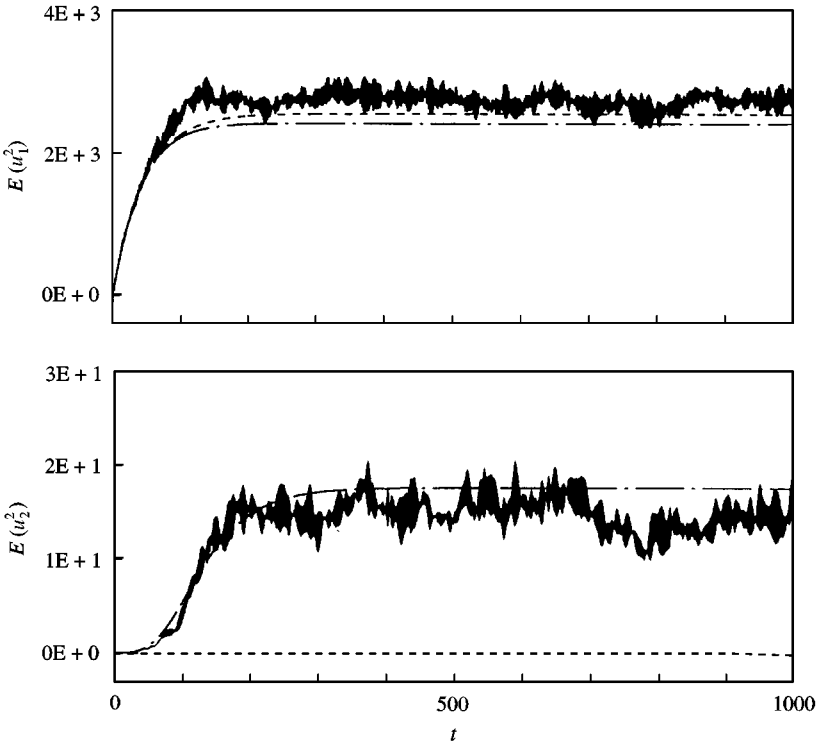


Figure 3. Mean-square time histories when the excitation is applied at the nodal point of the second mode ($c_1 = c_2 = c_3 = 100, \varepsilon = 0{\cdot}0001, 2\varepsilon^2 D = 1500$): ·····, Gaussian closure (2 modes); – – –, non-Gaussian closure (2 modes); —, Monte Carlo simulation (3 modes).

Substituting equations (15) and (16) into equations (14) we can obtain a system of 14 coupled differential equations which consist of four equations for the first order moments and 10 equations for the second order moments.

For non-Gaussian processes the cumulants of order higher than the second do not vanish. However, their contribution diminishes as their order increases if the process deviates slightly from Gaussian. Thus, the non-Gaussian closure is carried out by setting fifth and sixth order cumulants to zero and expressing fifth and sixth order moments in terms of lower order moments as follows:

$$
\begin{aligned}
E[X_{h_1}X_{h_2}X_{h_3}X_{h_4}X_{h_5}] = {} & \sum^{5} E[X_{h_1}]\,E[X_{h_2}X_{h_3}X_{h_4}X_{h_5}] \\
& - 2\sum^{10} E[X_{h_1}]\,E[X_{h_2}]\,E[X_{h_3}X_{h_4}X_{h_5}] \\
& + 6\sum^{10} E[X_{h_1}]\,E[X_{h_2}]\,E[X_{h_3}]\,E[X_{h_4}X_{h_5}] \\
& - 2\sum^{15} E[X_{h_1}]\,E[X_{h_2}X_{h_3}]\,E[X_{h_4}X_{h_5}]
\end{aligned}
$$

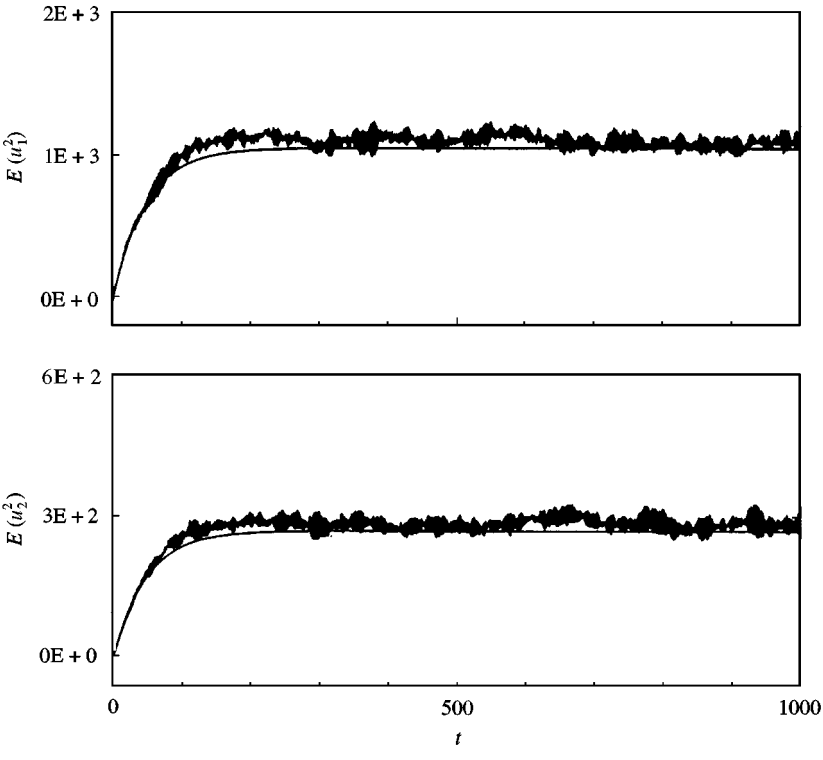


Figure 4. Mean-square time histories when the excitation is applied at the antinode of the second mode ($c_1 = c_2 = c_3 = 100, \varepsilon = 0{\cdot}0001, 2\varepsilon^2 D = 1500$): ·····, Gaussian closure (2 modes); – – –, non-Gaussian closure (2 modes); —, Monte Carlo simulation (3 modes).

$$+ \sum^{10} E[X_{h_1}X_{h_2}]\,E[X_{h_3}X_{h_4}X_{h_5}]$$

$$- 24E[X_{h_1}]\,E[X_{h_2}]\,E[X_{h_3}]\,E[X_{h_4}]\,E[X_{h_5}], \tag{17}$$

$$E[X_{h_1}X_{h_2}X_{h_3}X_{h_4}X_{h_5}X_{h_6}] = \sum^{6} E[X_{h_1}]\,E[X_{h_2}X_{h_3}X_{h_4}X_{h_5}X_{h_6}]$$

$$- 2\sum^{15} E[X_{h_1}]\,E[X_{h_2}]\,E[X_{h_3}X_{h_4}X_{h_5}X_{h_6}]$$

$$+ 6\sum^{20} E[X_{h_1}]\,E[X_{h_2}]\,E[X_{h_3}]\,E[X_{h_4}X_{h_5}X_{h_6}]$$

$$- 24\sum^{15} E[X_{h_1}]\,E[X_{h_2}]\,E[X_{h_3}]\,E[X_{h_4}]\,E[X_{h_5}X_{h_6}]$$

$$+ 6\sum^{45} E[X_{h_1}]\,E[X_{h_2}]\,E[X_{h_3}X_{h_4}]\,E[X_{h_5}X_{h_6}]$$

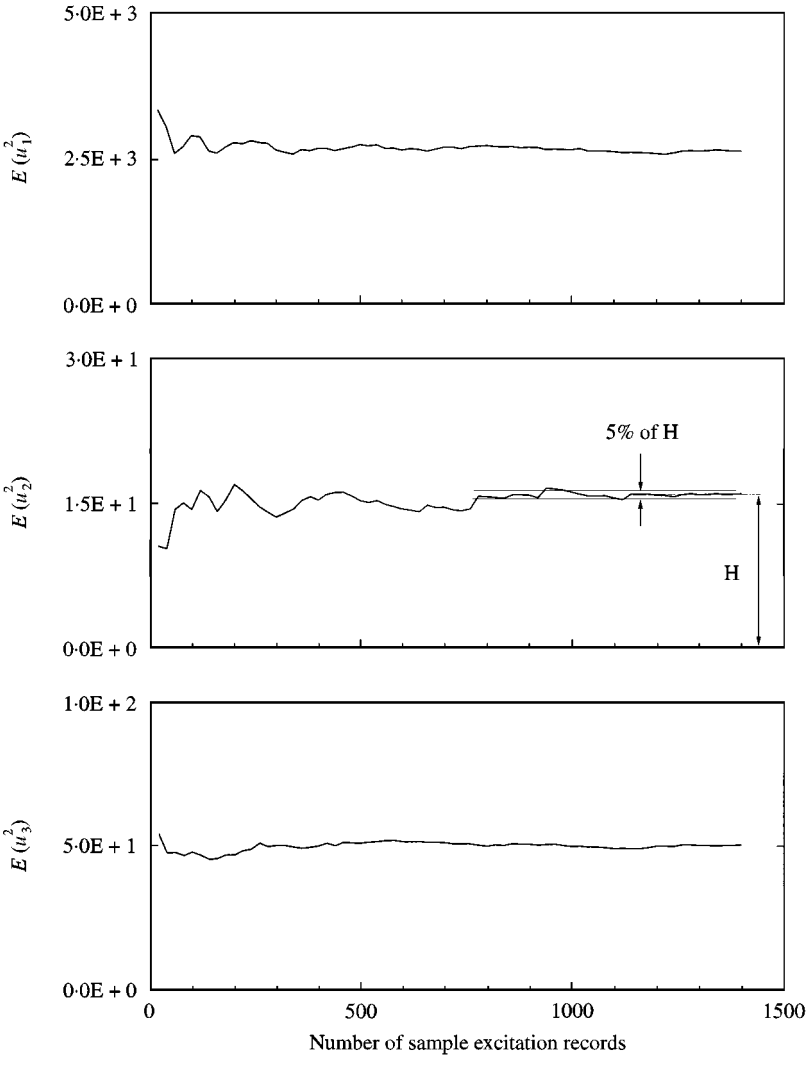


Figure 5. Mean-square responses at $t = 900$ versus the number of sample excitation records when the excitation is applied at the nodal point of the second mode ($c_1 = c_2 = c_3 = 100$, $\varepsilon = 0{\cdot}0001$, $2\varepsilon^2 D = 1500$).

$$+ \sum^{15} E[X_{h_1}X_{h_2}]\,E[X_{h_3}X_{h_4}X_{h_5}X_{h_6}]$$

$$+ \sum^{10} E[X_{h_1}X_{h_2}X_{h_3}]\,E[X_{h_4}X_{h_5}X_{h_6}]$$

$$- 2\sum^{15} E[X_{h_1}X_{h_2}]\,E[X_{h_3}X_{h_4}]\,E[X_{h_5}X_{h_6}]$$

$$- 2\sum^{60} E[X_{h_1}]\,E[X_{h_2}X_{h_3}]\,E[X_{h_4}X_{h_5}X_{h_6}]$$

$$- 120\,E[X_{h_1}]\,E[X_{h_2}]\,E[X_{h_3}]\,E[X_{h_4}]\,E[X_{h_5}]\,E[X_{h_6}]. \qquad (18)$$

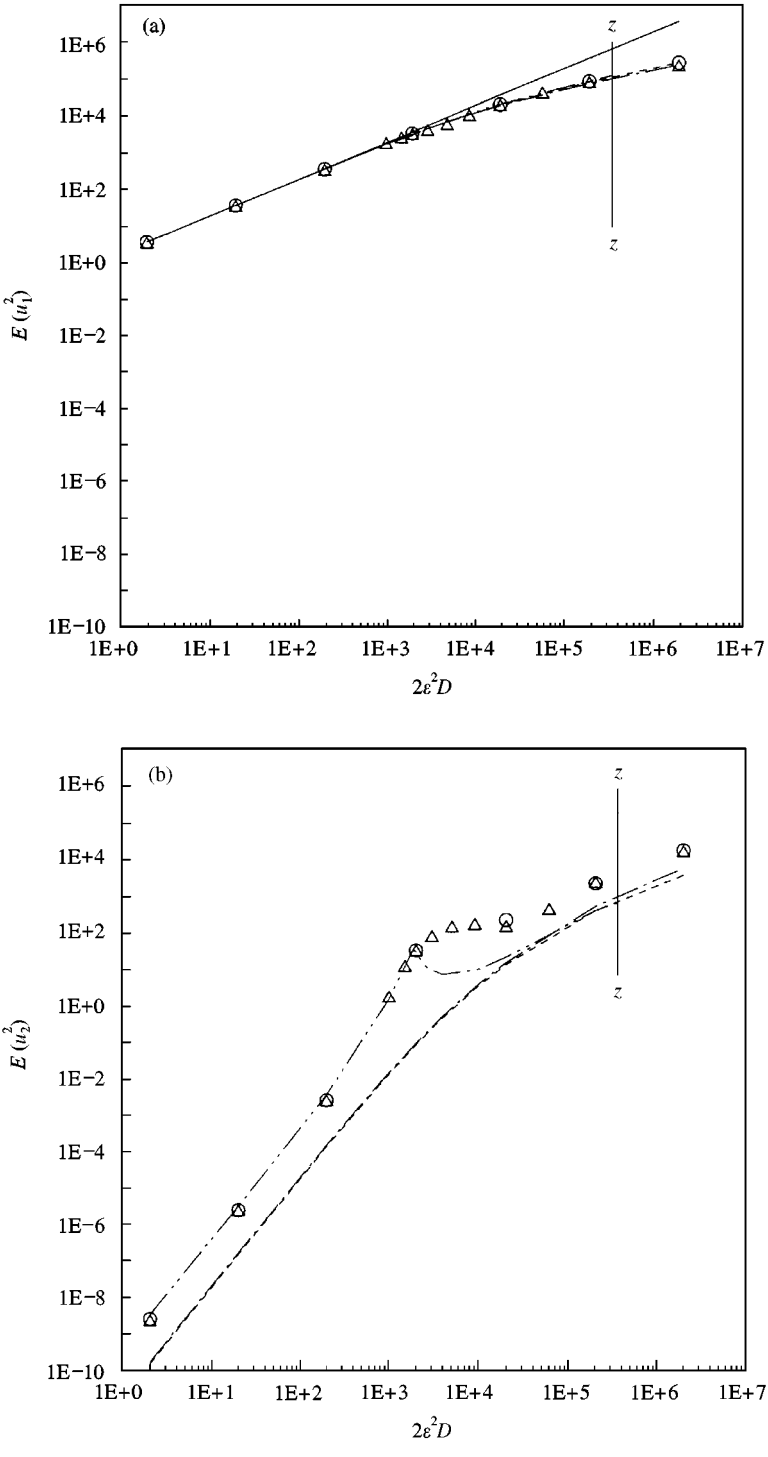


Figure 6. Mean-square responses versus spectral density $2\varepsilon^2 D$ when the excitation is applied at the nodal point of the second mode ($c_1 = c_2 = c_3 = 100$, $\varepsilon = 0{\cdot}0001$): —, linear; ·····, Gausian closure (2 modes); – - –, Gaussian closure (3 modes): — - - —, non-Gaussian closure (2 modes); ○, Monte Carlo simulation (2 modes); △, Monte Carlo simulation (3 modes). (a) First mode; (b) second mode; (c) third mode.

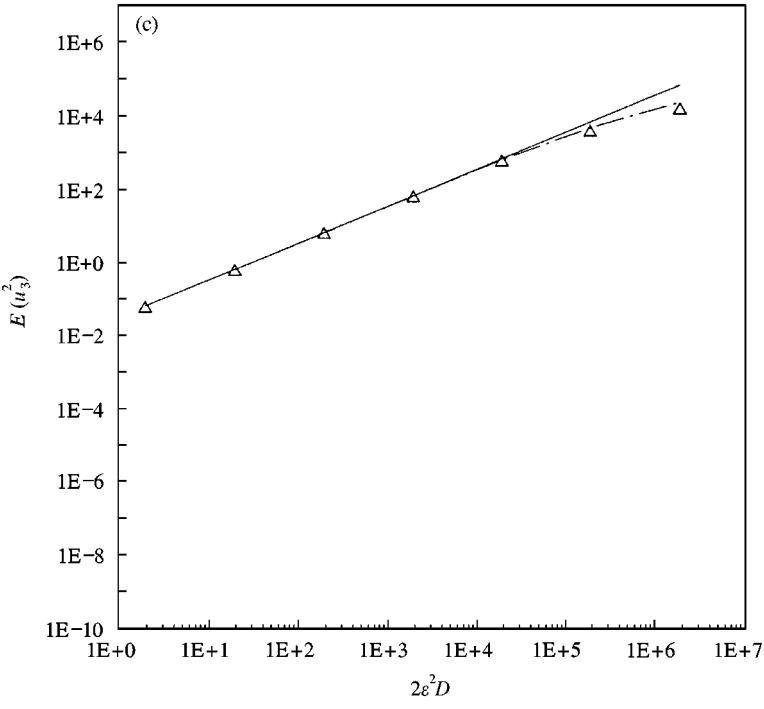


Figure 6. Continued.

In this case, we can obtain a system of 69 coupled differential equations which consist of four equations for the first order moments, 10 equations for the second order moments, 20 equations for the third order moments, and 35 equations for the fourth order moments.

For convenience the system is expressed as follows:

$$\mathbf{m}' = f(\mathbf{m}), \tag{19}$$

where $\mathbf{m} = \{m_{1,0,0,0,0,0}, m_{0,1,0,0,0,0}, \dots\}^{\mathrm{T}}$ is the moment vector consisting of 14 or 69 moments and $f(\mathbf{m}) = \{f_1(\mathbf{m}), f_2(\mathbf{m}), \dots\}^{\mathrm{T}}$ is the vector field of the system.

## 6. NUMERICAL RESULTS

We investigate the long-term behaviour of the moments by integrating numerically the ordinary differential equation (19) obtained by Gaussian and non-Gaussian closures.

Figures 3 and 4 show mean-square responses when the excitation is applied at the nodal point and the antinode of the second mode respectively. These two figures represent time histories of mean square responses corresponding to two-mode interaction by the Gaussian closure and the non-Gaussian closure, and three-mode interaction by Monte Carlo simulation for $c_1 = c_2 = c_3 = 100$. $\varepsilon = 0{\cdot}0001$, $2\varepsilon^2 D = 1500$. In Figure 3, the results from non-Gaussian closure and Monte Carlo simulation show the energy transfer between the first and second modes. The result from Gaussian closure does not agree with these. In Figure 4 results from two analytical schemes and Monte Carlo simulation agree very well and show energy transfer between two modes.

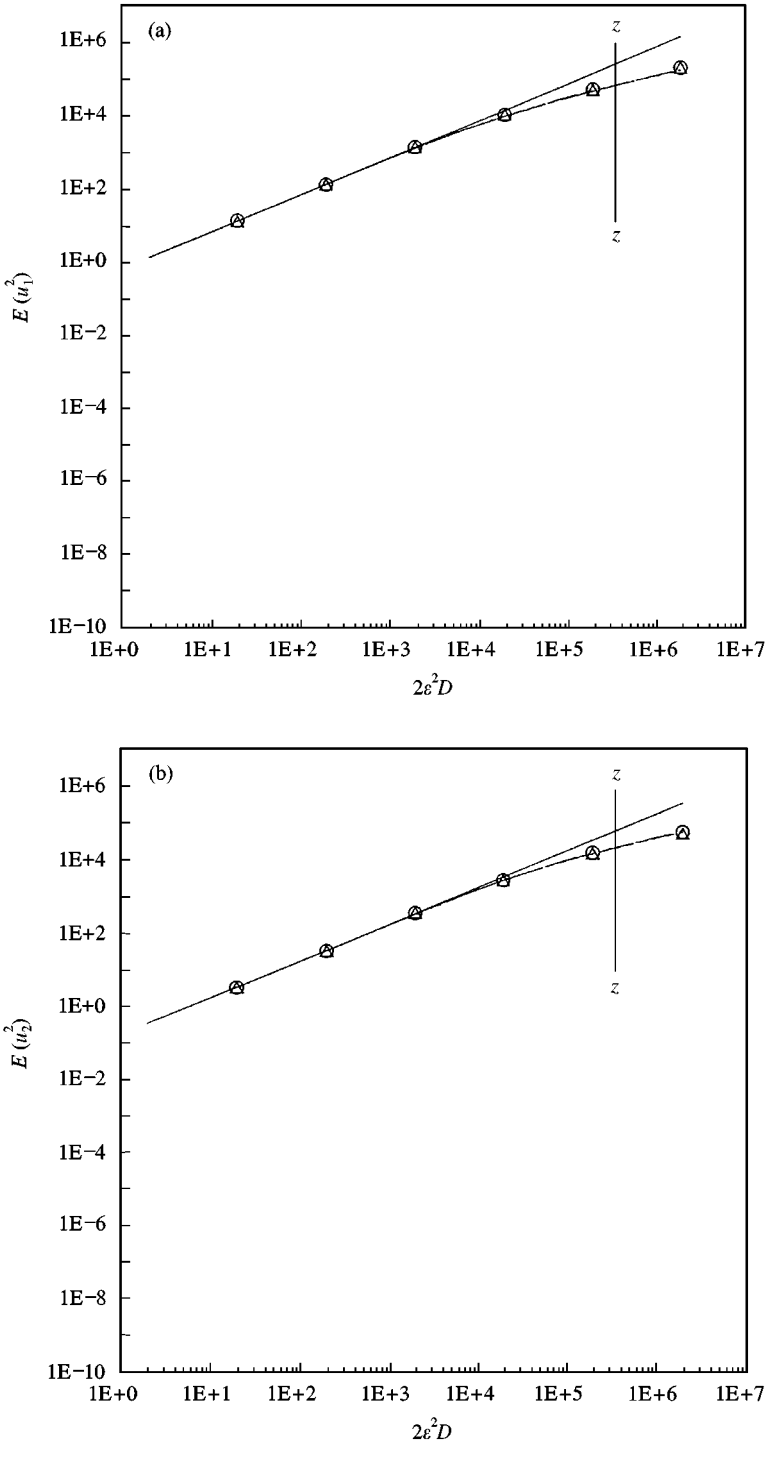


Figure 7. Mean-square responses versus spectral density $2\varepsilon^2 D$ when the excitation is applied at the antinode of the second mode ($c_1 = c_2 = c_3 = 100, \varepsilon = 0{\cdot}0001$): —, linear; ·····, Gaussian closure (2 modes); – – –, Gaussian closure (3 modes); — - - —, non-Gaussian closure (2 modes); ○, Monte Carlo simulation (2 modes); △, Monte Carlo simulation (3 modes). (a) First mode; (b) second mode; (c) third mode.

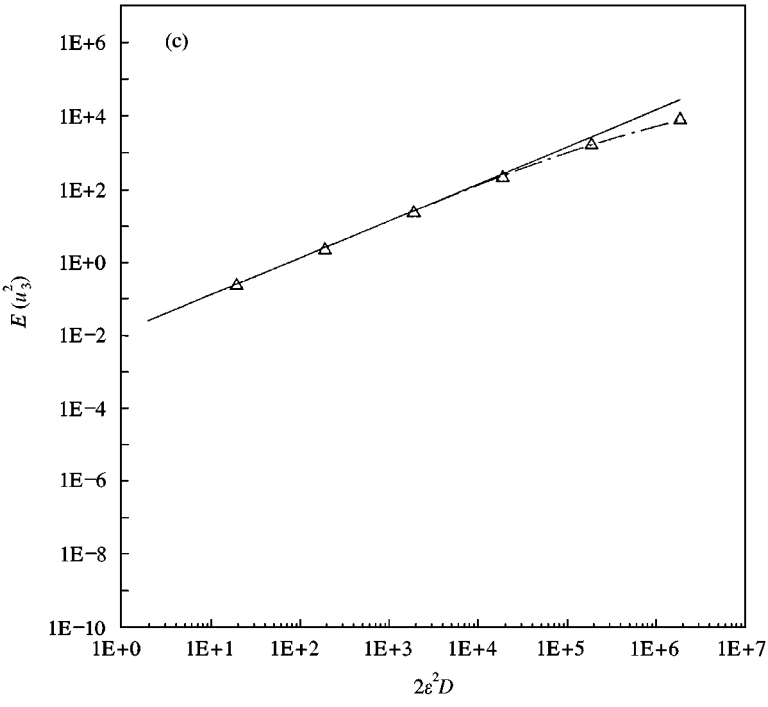


Figure 7. Continued.

For Monte Carlo simulation [16, 17], the response statistics are estimated by numerically integrating the non-linear coupled equations (5) for a large number of sample excitation records. In order to check the numerical convergence we plotted Figure 5, which shows that mean-square responses at a specific time depend on the number of sample excitation records. This figure shows that 1000 records are found to be adequate to give convergence of the results. The "H" in the figure represents temporal mean for mean-square responses between 1200 and 1400 of sample excitation records. Each record of the random excitation $W(t)$ with duration $t = 1000$ is generated by sampling a sequence of $N = 40\,000$ random numbers in order to prevent unacceptable frequency distortion in the record as follows:

$$W(t) = \sum_{j=1}^{N} \sqrt{2(4D_j)\ (f_{j+1} - f_j)}\, \sin(2\pi \sqrt{f_j f_{j+1}}\, t + \phi_j), \tag{20}$$

where $4D_j$ are one-sided spectral density, $f_j$ are random frequency, independent and uniformly distributed in ascending order [0, 20 Hz], and $\phi_j$ are random phase angles, independent and uniformly distributed on the interval $[0, 2\pi]$. The sampling time stepsize ($\Delta t$) is chosen to be less than $1/(2f_{max})$.

Figures 6 and 7 show mean-square responses in the steady state as functions of spectral density $2\varepsilon^2 D$ proportional to mean-square excitation $\sigma_W^2$ when the excitation is applied at the nodal point and the antinode of the second mode respectively. All of these figures except Figure 6(b) show that results from two analytical schemes and Monte Carlo simulation agree very well, and the result (solid line) from linear analysis agrees with these results especially when excitation level is low. In Figure 6(b) result from Monte Carlo simulation agrees with result from non-Gaussian closure rather than one from Gaussian closure as

expected from Figure 3. Result from linear analysis does not appear in the figure because the second mode is excited through non-linear coupling. In Figures 6(a), 6(b), 7(a), and 7(b) beyond the excitation level $z$–$z$ we cannot get any solution by the non-Gaussian closure scheme because the solution experiences divergence. Comparing results from two- and three-mode interactions we can conclude that there exists no significant difference between both modal interactions.

## 7. CONCLUSIONS

An analysis has been presented for the modal interactions of a hinged–clamped beam under broadband random excitation. By means of internal resonance conditions two- and three-mode interactions are considered. The energy transfer from the first and third modes excited directly to the second mode excited indirectly through non-linear coupling has been found. It is also observed that in some case result from Monte Carlo simulation agrees with result from non-Gaussian closure rather than one from Gaussian closure. Analytical and numerical results show that there exists no significant difference between two- and three-mode interactions.

## ACKNOWLEDGMENT

This work was supported by the Korea Science and Engineering Foundation under Grant KOSEF 96-0200-07-01-3.

## REFERENCES

1. W. Y. Tseng and J. Dugundji 1970 *ASME Journal of Applied Mechanics* **37**, 292–297. Non-linear vibrations of a beam under harmonic excitation.
2. S. Atluri 1973 *ASME Journal of Applied Mechanics* **40**, 121–126. Nonlinear vibrations of a hinged beam including non-linear inertia effects.
3. C. L. Lou and D. L. Sikarskie 1975 *ASME Journal of Applied Mechanics* **42**, 209–214. Nonlinear vibration of beams using a form-function approximation.
4. R. Lewandowski 1987 *Journal of Sound and Vibration* **114**, 91–101. Application of the Ritz method to the analysis of nonlinear free vibrations of beams.
5. A. H. Nayfeh, D. T. Mook and S. Sridhar 1974 *Journal of Acoustical Society of America* **55**, 281–291. Nonlinear analysis of the forced response of structural elements.
6. S. Sridhar, A. H. Nayfeh and D. T. Mook 1975 *Journal of Acoustical Society of America* **58**, 113–123. Nonlinear resonances in a class of multi-degree-of-freedom systems.
7. A. H. Nayfeh and D. T. Mook 1979 *Nonlinear Oscillations*. New York: John Wiley & Sons Inc.
8. W. K. Lee and K. Y. Soh 1994 *Nonlinear Dynamics* **6**, 49–68. Nonlinear analysis of the forced response of a beam with three mode interaction.
9. W. K. Lee and M. R. Ghang 1994 *ASME Journal of Applied Mechanics* **61**, 144–151. Domains of attraction of a forced beam by interpolated mapping.
10. W. K. Lee and C. H. Kim 1997 *Nonlinear Dynamics* **14**, 37–48. Evolution of domains of attraction of a forced beam with two-mode interaction.
11. R. A. Ibrahim, B. H. Lee and A. A. Afaneh 1993 *ASME Journal of Vibration and Acoustics* **115**, 193–201. Structural modal multifurcation with internal resonance—part 2: stochastic approach.
12. B. H. Lee and R. A. Ibrahim 1994 *Probabilistic Engineering Mechanics* **9**, 23–32. Stochastic bifurcation in non-linear structural systems near 1 : 1 internal resonance.
13. T. T. Soong 1973 *Random Differential Equations in Science and Engineering*. New York: Academic Press Inc.
14. R. A. Ibrahim 1985 *Parametric Random Vibration*. New York: John Wiley & Sons Inc.

15. Y. K. LIN and G. Q. CAI 1995 *Probabilistic Structural Dynamics Advanced Theory and Application.* New York: McGraw-Hill, Inc.
16. M. SHINOZUKA and G. DEODATIS 1991 *Applied Mechanics Review* **44**, 191–204. Simulation of stochastic processes by spectral representation.
17. C. Y. YANG 1986 *Random Vibration of Structures.* New York: John Wiley & Sons Inc.